



Published in final edited form as:

*Liver Res.* 2020 September ; 4(3): 136–144. doi:10.1016/j.livres.2020.08.004.

## Adoptive transfer of *Pfkfb3*-disrupted hematopoietic cells to wild-type mice exacerbates diet-induced hepatic steatosis and inflammation

Xin Guo<sup>a,b</sup>, Bilian Zhu<sup>a,c</sup>, Hang Xu<sup>a</sup>, Honggui Li<sup>a</sup>, Boxiong Jiang<sup>c</sup>, Yina Wang<sup>c</sup>, Benrong Zheng<sup>c</sup>, Shannon Glaser<sup>d</sup>, Gianfranco Alpini<sup>e,f</sup>, Chaodong Wu<sup>a,\*</sup>

<sup>a</sup>Department of Nutrition, Texas A&M University, College Station, TX, USA

<sup>b</sup>Department of Nutrition and Food Hygiene, School of Public Health, Cheeloo College of Medicine, Shandong University, Jinan, China

<sup>c</sup>Department of VIP Medical Service Center, The Third Affiliated Hospital of Sun Yat-sen University, Guangzhou, China

<sup>d</sup>Medical Physiology, Texas A&M University College of Medicine, Bryan, TX, USA

<sup>e</sup>Hepatology and Gastroenterology, Medicine, Indiana University, Indianapolis, IN, USA

<sup>f</sup>Richard L. Roudebush VA Medical Center, Indianapolis, IN, USA

### Abstract

**Background and objectives:** Hepatic steatosis and inflammation are key characteristics of non-alcoholic fatty liver disease (NAFLD). However, whether and how hepatic steatosis and liver inflammation are differentially regulated remains to be elucidated. Considering that disruption of 6-phosphofructo-2-kinase/fructose-2,6-biphosphatase 3 (*Pfkfb3*/*Pfk2*) dissociates fat deposition and inflammation, the present study examined a role for *Pfkfb3*/*Pfk2* in hematopoietic cells in regulating hepatic steatosis and inflammation in mice.

**Methods:** *Pfkfb3*-disrupted (*Pfkfb3*<sup>+/-</sup>) mice and wild-type (WT) littermates were fed a high-fat diet (HFD) and examined for NAFLD phenotype. Also, bone marrow cells isolated from *Pfkfb3*<sup>+/-</sup> mice and WT mice were differentiated into macrophages for analysis of macrophage activation status and for bone marrow transplantation (BMT) to generate chimeric (WT/BMT- *Pfkfb3*<sup>+/-</sup>) mice in which *Pfkfb3* was disrupted only in hematopoietic cells and control chimeric (WT/BMT-WT) mice. The latter were also fed an HFD and examined for NAFLD phenotype. *In vitro*,

This is an open access article under the CC BY-NC-ND license (<http://creativecommons.org/licenses/by-nc-nd/4.0/>).

\*Corresponding author. Department of Nutrition, Texas A&M University, College Station, TX, USA. cdwu@tamu.edu (C. Wu). Authors' contributions

X. Guo, B. Zhu, and H. Xu contributed equally to this study. X. Guo, B. Zhu, and H. Xu carried out most of experiments involving mice. B. Zhu and H. Li carried out most of the experiments involving cells. X. Guo, B. Zhu, H. Xu, and H. Li collected tissue and cell samples and performed molecular and biochemical assays. H. Li performed histological assays. B. Jiang, Y. Wang, B. Zheng, S. Glaser, and G. Alpini contributed to data analysis and scientific discussion. C. Wu came up the concept of the study and supervised all experiments and wrote the manuscript.

Declaration of competing interest

The authors declare that they have no conflict of interest.

hepatocytes were co-cultured with bone marrow-derived macrophages and examined for hepatocyte fat deposition and proinflammatory responses.

**Results:** After the feeding period, HFD-fed *Pfkfb3*<sup>3+/-</sup> mice displayed increased severity of liver inflammation in the absence of hepatic steatosis compared with HFD-fed WT mice. When inflammatory activation was analyzed, *Pfkfb3*<sup>3+/-</sup> macrophages revealed increased proinflammatory activation and decreased anti-proinflammatory activation. When NAFLD phenotype was analyzed in the chimeric mice, WT/BMT-*Pfkfb3*<sup>3+/-</sup> mice displayed increases in the severity of HFD-induced hepatic steatosis and inflammation compared with WT/BMT-WT mice. At the cellular level, hepatocytes co-cultured with *Pfkfb3*<sup>3+/-</sup> macrophages revealed increased fat deposition and proinflammatory responses compared with hepatocytes co-cultured with WT macrophages.

**Conclusions:** *Pfkfb3* disruption only in hematopoietic cells exacerbates HFD-induced hepatic steatosis and inflammation whereas the *Pfkfb3*/iPfk2 in nonhematopoietic cells appeared to be needed for HFD feeding to induce hepatic steatosis. As such, the *Pfkfb3*/iPfk2 plays a unique role in regulating NAFLD pathophysiology.

### Keywords

6-Phosphofructo-2-kinase/fructose-2,6-biphosphatase 3 (Pfkfb3/iPfk2); Hematopoietic cells; Hepatic steatosis; Inflammation; Macrophages

## 1. Introduction

Non-alcoholic fatty liver disease (NAFLD) is characterized by hepatic steatosis and progresses to non-alcoholic steatohepatitis (NASH). The latter is the advanced form of NAFLD where the liver displays overt inflammatory damages. Various epidemiological studies have demonstrated that obesity increases the incidence of NAFLD by 7–10 fold.<sup>1,2</sup> Accordingly, obesity-associated metabolic abnormalities, such as chronic low-grade inflammation, adiposity, and insulin resistance, are considered as key factors contributing to the development and progression of NAFLD. Indeed, recent research has advanced the understanding of how obesity-associated inflammation triggers or exacerbates the pathogenesis of NAFLD. For instance, a number of metabolic and inflammatory pathways within macrophages, a major type of immune cells that regulates NAFLD phenotype, have been validated to either activate or suppress macrophage activation and act through paracrine manners to alter hepatocyte metabolic and inflammatory responses and hepatic stellate cell activation status.<sup>3–8</sup> During NASH, monocyte-derived macrophages also have been implicated as a major type of cells accounting for liver inflammation and fibrosis.<sup>9,10</sup> In addition, obesity-associated adipose tissue dysfunction is accepted to deliver excessive amount of fat flow and adipokines to the liver, which in turn acts on liver cells including hepatocytes and macrophages to promote NAFLD.<sup>11–13</sup> Although the mechanisms underlying obesity-associated adipose tissue dysfunction remain to be elucidated, increased proinflammatory activation of macrophages within adipose tissue is considered as a causal factor accounting for adipose tissue dysfunction. Clearly, macrophages are of particular importance in the pathogenesis of NAFLD.

As it is well established in mice, feeding a high-fat diet (HFD) induces inflammation in the liver and adipose tissue, along with hepatic steatosis, increased adiposity, and systemic insulin resistance.<sup>6,14</sup> However, there also is increasing evidence that indicates the dissociation between fat deposition and increased insulin resistance and inflammatory responses. For instance, targeted overexpression of human acyl-CoA:diacylglycerol acyltransferase (DGAT) in the liver causes hepatic steatosis, but not glucose intolerance and systemic insulin resistance.<sup>15</sup> In this line of transgenic mice, the liver also displays normal inflammatory responses.<sup>15</sup> Similarly, supplementation of palmitoleate, a monounsaturated fatty acid whose circulating levels are positively correlated with hepatic steatosis,<sup>16,17</sup> increases hepatic steatosis while suppressing liver proinflammatory responses.<sup>18</sup> The mechanisms underlying the dissociation of inflammation and fat deposition remain to be elucidated, and warrant careful considerations of how inflammation versus fat deposition as critical obesity-associated factors separately contribute to the pathogenesis of NAFLD.

As one of the four *Pfkfb* genes, *Pfkfb3* encodes the inducible 6-phosphofructo-2-kinase (iPfk2).<sup>19,20</sup> The latter generates fructose-2,6-bisphosphate (F2,6P<sub>2</sub>), which in turn acts as the most powerful activator of glycolytic enzyme 6-phosphofructo-1-kinase (6Pfk1).<sup>19,21</sup> It has been documented that among the key tissues that are involved in the regulation of systemic insulin sensitivity and metabolic homeostasis, adipose tissue has high abundance of *Pfkfb3*/iPfk2 whereas the liver and skeletal muscle have very low levels of *Pfkfb3*/iPfk2.<sup>22</sup> Also, previous evidence has demonstrated a critical role for *Pfkfb3*/iPfk2 in dissociating HFD-induced adiposity from proinflammatory responses in mice whose *Pfkfb3* was disrupted.<sup>22</sup> Specifically, *Pfkfb3* disruption ameliorated HFD-induced adiposity but exacerbated the proinflammatory responses in adipose tissue. In contrast, adipocyte-specific overexpression of *Pfkfb3*/iPfk2 markedly increased the degree of HFD-induced adiposity while decreasing adipose tissue inflammation. Notably, this line of mice displayed increased hepatic steatosis while revealing decreased liver inflammation and increased hepatic insulin sensitivity. Given this, the *Pfkfb3*/iPfk2 in adipocytes appears to play a unique role in the pathogenesis of NAFLD. Since *Pfkfb3*/iPfk2 is also expressed at high abundance in macrophages, a recent study examined NAFLD phenotype in mice whose *Pfkfb3* was disrupted only in myeloid cells, and suggested that the *Pfkfb3*/iPfk2 in myeloid cells, unlike that in adipocytes, appears to act through suppressing macrophage proinflammatory activation to protect against HFD-induced NAFLD.<sup>23</sup> In particular, the *Pfkfb3* in macrophages is not just to regulate the rates of glycolysis, but more broadly to coordinate overall metabolic homeostasis, thereby determining macrophage activation. Given the importance of macrophages in NAFLD pathophysiology, the present study examined HFD-induced NAFLD phenotype in global *Pfkfb3*-disrupted mice and in chimeric mice in which *Pfkfb3* was disrupted only in hematopoietic cells. The results verified a role for macrophage *Pfkfb3* in protecting against diet-induced NAFLD.

## 2. Materials and methods

### 2.1. Ethical approval

All study protocols were reviewed and approved by the Institutional Animal Care and Use Committee of Texas A&M University.

## 2.2. Animal experiments

Wild-type (WT) C57BL/6J mice were obtained from The Jackson Laboratory (Bar Harbor, ME, USA). Global heterozygous *Pfkfb3*-disrupted (*Pfkfb3*<sup>+/-</sup>) mice were generated and maintained as previously described (homozygous *Pfkfb3* disruption is embryonic lethal).<sup>22,24</sup> All mice were maintained on a 12:12-h light-dark cycle (lights on at 06:00). All mice were fed *ad libitum* except those that were used for dietary feeding study. Study 1 (global *Pfkfb3* disruption on NAFLD phenotype): male *Pfkfb3*<sup>+/-</sup> mice and WT littermates, at 5–6 weeks of age, were fed an HFD (60% fat calories, 20% carbohydrate calories, and 20% protein calories; Research Diets, Inc.) or low-fat diet (LFD, 10% fat calories, 70% carbohydrate calories, and 20% protein calories) for 12 weeks as previously described.<sup>22,25,26</sup> Study 2 (hematopoietic cell-specific *Pfkfb3* disruption on NAFLD phenotype): to generate chimeric mice in which *Pfkfb3* was disrupted only in hematopoietic cells, male WT mice, at 5–6 weeks of age, were subjected to bone marrow transplantation (BMT) as described below. After recovery, chimeric mice were fed an HFD for 12 weeks as described in Study 1. After the feeding period, mice in both studies were fasted for 4 h prior to collection of blood and tissue samples.<sup>7,26</sup> After weighing, liver samples were either fixed and embedded for histological and immunohistochemical analyses or frozen in liquid nitrogen and then stored at -80 °C for further analyses. Some male mice were fed *ad libitum* and subjected to isolation of bone marrow cells as described below.

## 2.3. Isolation of bone marrow cells and differentiation of macrophages

Bone marrow cells were isolated from the tibias and femurs of male *Pfkfb3*<sup>+/-</sup> mice and its WT littermates, at 8–10 weeks of age as described.<sup>5,7</sup> After erythrocyte lysis with ammonium chloride (Stem Cell Technologies, Cambridge, MA, USA), cells were either used for BMT or induced for differentiation with Iscove's modified Dulbecco's medium containing 10% fetal bovine serum (FBS) and 15% L929 culture supernatant for 8 days. The bone marrow-derived macrophages (BMDMs) were analyzed for its activation status or used for the co-culture study.

## 2.4. BMT

BMT was performed as previously described.<sup>5,7</sup> At 5–6 weeks of age, male WT recipients were lethally irradiated and transplanted with bone marrow cells from *Pfkfb3*<sup>+/-</sup> mice and/or WT littermates. WT/BMT-*Pfkfb3*<sup>+/-</sup> mice, in which *Pfkfb3* was disrupted only in hematopoietic cells, and WT/BMT-WT mice, in which *Pfkfb3* was intact in all cells, were allowed to recover for 4 weeks. After recovery, the chimeric mice were fed an HFD for 12 weeks and subjected to metabolic assays and tissue collections.

## 2.5. Histological and immunohistochemical analyses

Paraffin-embedded mouse liver blocks were cut into sections of 5 μm thickness and stained with hematoxylin and eosin (H&E) and/or stained for F4/80 expression with rabbit anti-F4/80 antibodies (1:100) (AbD Serotec, Raleigh, NC, USA).<sup>6,23</sup> The fraction of F4/80-expressing cells for each sample is calculated as the sum of the number of nuclei of F4/80-expressing cells divided by the total number of nuclei in sections of a sample. Six fields per

slide were included, and a total of 4–6 mice per group were used. Frozen liver sections (4–5  $\mu\text{m}$  thick) were stained with Oil Red O as described.<sup>6</sup>

## 2.6. Cell culture and treatment

After differentiation, BMDMs were harvested and examined for *Pfkfb3* expression using real-time polymerase chain reaction (PCR). Upon validating *Pfkfb3* disruption, additional BMDMs were subjected to metabolic and inflammatory assays. To quantify glycolysis rates, each well (6-well plate) of BMDMs were incubated with medium supplemented with 1  $\mu\text{Ci}$  [ $3\text{-}^3\text{H}$ ]-glucose for 3 h. After incubation, the medium was collected to determine the production of  $^3\text{H}_2\text{O}$  (in disintegration per minute (DPM)) as described.<sup>27</sup> Rates of glycolysis were calculated as nanomoles of glucose metabolized per 3 h per milligram of protein and normalized to the average of control. To analyze macrophage proinflammatory signaling, lysates of BMDMs were subjected to Western blot analysis. Additional BMDMs were treated with lipopolysaccharide (LPS, 20 ng/mL) for 6 h prior to harvest to examine the expression of interleukin-1beta (*Il-1b*), *Il-6*, and tumor necrosis factor alpha (*Tnfa*). To analyze macrophage anti-inflammatory activation, some BMDMs were treated with or without Il-4 (10 ng/mL) in the presence or absence of pioglitazone (Pio, 1  $\mu\text{M}$ ) for 48 h and examined for the expression of *Il-1b* and *Il-6* or protein amount of Arginase 1 and peroxisome proliferator-activated receptor gamma (Pparg), which all are indicators of macrophage alternative activation.<sup>28,29</sup> Additional BMDMs were subjected to hepatocyte-macrophage co-culture study as described below.

Primary hepatocytes were isolated from free-fed male WT C57BL/6J mice, at 8–10 weeks of age, as described.<sup>6</sup> After attachment, hepatocytes were further incubated in M199 supplemented with 10% FBS and 100 U/mL penicillin and 100  $\mu\text{g}/\text{mL}$  streptomycin for 24 h. For hepatocyte-macrophage co-culture study, bone marrow cells were prepared from *Pfkfb3*<sup>+/-</sup> mice and WT littermates, as well as *Myc-Pfkfb3*<sup>+/-</sup> mice and *Myc-Pfkfb3*<sup>+/+</sup> mice as described,<sup>23</sup> at 6 days prior to hepatocyte isolation. After differentiation, BMDMs were trypsinized and added to WT primary mouse hepatocytes at a ratio of 1:10 as described.<sup>6,30</sup> The co-cultures were incubated with fresh media for 48 h and treated with palmitate (250  $\mu\text{M}$ ) or BSA for the last 24 h and assessed for fat deposition or incubated for 48 h in the absence or presence of LPS (100 ng/mL) for the last 30 min to examine inflammatory signaling.

## 2.7. Biochemical and molecular assays

To determine liver inflammatory signaling, lysates of frozen livers were subjected to Western blot analysis to measure total amount and/or phosphorylation states of nuclear factor kappa B (Nfkb) p65 as described.<sup>6,31</sup> Similarly, to analyze liver insulin signaling, liver lysates were examined for the total amount and phosphorylation states of Akt using Western blot analysis.<sup>6,31</sup> All primary antibodies were from Cell Signaling Technology (Danvers, MA, USA). The maximum intensity of each band was quantified using Image J software. To determine gene expression, the total RNA was isolated from cultured/isolated cells, and subjected to reverse transcription and real-time PCR analysis. Results were normalized to 18s ribosomal RNA and plotted as relative expression to the average of WT or PBS-treated WT, which was set as 1. To assess hepatocyte fat deposition, the co-cultures of hepatocytes

and macrophages were treated with or without palmitate for 24 h. At 1 h prior to harvest, the cells were stained with Oil Red O and quantified for fat content as described.<sup>6,12</sup>

## 2.8. Statistical analysis

Numeric data are presented as means  $\pm$  standard error of the mean (SEM). Statistical significance was determined using unpaired, two-tailed ANOVA or Student's *t* tests. Differences were considered significant at the two-tailed  $P < 0.05$ .

## 3. Results

### 3.1. Global *Pfkfb3* disruption blunts HFD-induced hepatic steatosis in mice

We have previously shown that global *Pfkfb3* disruption ameliorates HFD-induced adiposity while increasing adipose tissue proinflammatory responses.<sup>22</sup> The same lines of mice (Fig. 1A) were examined for HFD-induced NAFLD phenotype. As described,<sup>22</sup> HFD-*Pfkfb3*<sup>+/-</sup> mice revealed smaller increases in body weight and visceral fat mass compared with HFD-WT mice (Fig. 1B). Moreover, HFD-*Pfkfb3*<sup>+/-</sup> mice displayed significantly decreased liver/body weight ratios compared with HFD-WT mice (Fig. 1C). When liver sections were examined, HFD-*Pfkfb3*<sup>+/-</sup> mice did not display hepatic steatosis whereas HFD-WT mice exhibited overt hepatic steatosis (Fig. 1D). However, in the absence of hepatic steatosis, HFD-*Pfkfb3*<sup>+/-</sup> mice revealed significantly more F4/80-positive cells in the liver compared with HFD-WT mice (Fig. 1D). These results suggest that *Pfkfb3* disruption dissociates hepatic steatosis and liver inflammation.

### 3.2. *Pfkfb3* disruption decreases macrophage glycolysis

How *Pfkfb3* disruption dissociates hepatic steatosis and liver inflammation is unknown, but may be attributable to cell-type-specific roles played by *Pfkfb3* in different cells, *e.g.*, adipocytes and macrophages. Since *Pfkfb3* is expressed at highly abundance in macrophages, we sought to explore a role for macrophage *Pfkfb3* in NAFLD pathophysiology. Initially, we quantified the rates of glycolysis in macrophages differentiated from bone marrow cells isolated from *Pfkfb3*<sup>+/-</sup> mice and its WT littermates. After validating *Pfkfb3* disruption (Fig. 2A), *Pfkfb3*<sup>+/-</sup> BMDMs, along with control BMDMs were examined for the rates of glycolysis. Indicated by the production of <sup>3</sup>H<sub>2</sub>O from BMDMs incubated with <sup>3</sup>-[H]-glucose, the rates of glycolysis in *Pfkfb3*<sup>+/-</sup> BMDMs were significantly lower than those in WT BMDMs (Fig. 2B). These results verified an essential role for *Pfkfb3* in regulating glycolysis in macrophages, and enabled us to address *Pfkfb3* regulation of macrophage activation in relation to NAFLD phenotype (see below).

### 3.3. *Pfkfb3* disruption increases macrophage proinflammatory activation and decreases macrophage anti-inflammatory activation

Homozygous *Pfkfb3* disruption exacerbates LPS-induced macrophage proinflammatory activation.<sup>23</sup> A similar finding was observed in the present study using macrophages prepared from *Pfkfb3*<sup>+/-</sup> mice as indicated by increased phosphorylation states of Nfkb p65, as well as mRNA levels of proinflammatory cytokines (LPS-stimulated *Il-1b* and *Tnf $\alpha$* ) (Fig. 3A and B). Next, the present study examined *Pfkfb3* regulation of macrophage anti-inflammatory activation. Under Il-4/Pio-stimulated conditions, the amount of Arginase 1 and

Pparg was increased significantly in WT BMDMs, but not or to a smaller extent in *Pfkfb3*<sup>+/-</sup> BMDMs (Fig. 3C). Similarly, under both basal and Il-4-stimulated condition, the mRNA levels of *Il-1b* and *Il-6* in *Pfkfb3*<sup>+/-</sup> BMDMs were significantly higher than their respective levels in WT BMDMs (Fig. 3D). Together, these results indicate that *Pfkfb3* disruption leads to increased macrophage proinflammatory activation and decreased macrophage anti-inflammatory activation.

#### 3.4. *Pfkfb3* disruption in hematopoietic cells exacerbates diet-induced hepatic steatosis and inflammation without altering body weight and adiposity

Myeloid cell-specific *Pfkfb3* disruption in mice exacerbates diet-induced hepatic steatosis and inflammation in the absence of altering body weight and adiposity.<sup>23</sup> For the current study, we used BMT as an alternative approach to verify the role of *Pfkfb3* in myeloid cells in regulating diet-induced phenotype in mice. During the feeding period, WT/BMT-*Pfkfb3*<sup>+/-</sup> mice and WT/BMT-WT mice consumed comparable amount of food (data not shown). Also, the body weight of WT/BMT-*Pfkfb3*<sup>+/-</sup> mice, before or after HFD feeding, did not differ significantly from that of WT/BMT-WT mice (Fig. 4A). Consistently, adiposity, calculated as the ratio of visceral fat mass to body weight, was comparable between the two groups of chimeric mice after HFD feeding (Fig. 4B). These results confirm that *Pfkfb3* disruption in hematopoietic cells does not alter body weight and adiposity of the chimeric mice.

When NAFLD phenotype was examined, HFD-fed WT/BMT-*Pfkfb3*<sup>+/-</sup> mice and HFD-fed WT/BMT-WT mice revealed comparable amount of liver weight and similar ratios of liver weight to body weight (Fig. 4C). However, the severity of hepatic steatosis in HFD-fed WT/BMT-*Pfkfb3*<sup>+/-</sup> mice was significantly greater than that in HFD-fed WT/BMT-WT mice, indicated by the results from liver sections stained with H&E and Oil Red O (Fig. 4D). Additionally, the numbers of hepatic F4/80-positive cells and liver phosphorylation of states of Nfkb p65 in HFD-fed WT/BMT-*Pfkfb3*<sup>+/-</sup> mice were significantly greater than their respective levels in HFD-fed WT/BMT-WT mice (Fig. 4D and E), indicating increased severity of liver inflammation in mice whose *Pfkfb3* was disrupted only in hematopoietic cells. Collectively, these results suggest that *Pfkfb3* disruption in hematopoietic cells exacerbates diet-induced hepatic steatosis and inflammation.

#### 3.5. Macrophage factors generated in response to *Pfkfb3* disruption promote hepatocyte fat deposition and proinflammatory cytokine expression

To verify a role for the *Pfkfb3* in macrophages in regulating hepatocyte events related to NAFLD, we performed macrophage-hepatocyte co-cultures. Upon palmitate stimulation, hepatocytes co-cultured with *Pfkfb3*<sup>+/-</sup> BMDMs revealed a significant increase in fat deposition compared with hepatocytes co-cultured with control BMDMs (Fig. 5A). Additionally, hepatocytes co-cultured with *Pfkfb3*<sup>+/-</sup> BMDMs revealed significantly increased phosphorylation states of Nfkb p65 under both basal and LPS-stimulated conditions (Fig. 5B). These results suggest that *Pfkfb3* disruption promotes macrophage generation of factors that act to enhance hepatocyte fat deposition and proinflammatory responses.

### 3.6. *Pfkfb3* disruption in hematopoietic cells impairs liver insulin signaling

Hepatic insulin resistance not only is a consequence of NAFLD, but also serves as a factor to increase hepatic lipogenesis. Next, the present study analyzed liver insulin signaling in HFD-fed chimeric mice. In HFD-fed WT/BMT-WT mice, insulin induced a significant increase in liver phosphorylation states of Akt (Fig. 6A and B). This effect of insulin, however, was weakened in livers of HFD-fed WT/BMT-*Pfkfb3*<sup>+/-</sup> mice. Therefore, *Pfkfb3* disruption in hematopoietic cells decreases liver insulin sensitivity.

## 4. Discussion

Obesity-associated adiposity, along with adipose tissue dysfunction, critically promotes the development and progression of one or more features of NAFLD.<sup>32-35</sup> Meanwhile, obesity-associated inflammation also plays an important role in regulating the pathogenesis of NAFLD.<sup>6,7,23</sup> Since increasing evidence has indicated the existence of dissociation of inflammation and fat deposition, it is critical to elucidate whether and how different aspects of obesity, *e.g.*, inflammation versus fat deposition, differentially regulate hepatic steatosis and inflammation. In the present study, we examined NAFLD phenotypes in global *Pfkfb3*-disrupted mice and in chimeric mice in which *Pfkfb3* was disrupted only in hematopoietic cells. Our results indicated that inflammation derived from *Pfkfb3*-disrupted hematopoietic cells plays a detrimental role in increasing the severity of HFD-induced hepatic steatosis and inflammation although the *Pfkfb3* in nonhematopoietic cells is needed for HFD to induce hepatic steatosis in mice. Using a co-culture system, we further validated that *Pfkfb3*-disrupted macrophages act on hepatocytes to increase palmitate-induced fat deposition and LPS-stimulated hepatocyte proinflammatory responses. As such, *Pfkfb3* plays a unique role in the development and progression of NAFLD.

As a regulatory gene of glycolysis, *Pfkfb3* regulates adipocyte metabolic and proinflammatory responses, in large part, through promoting glycolysis and glycolysis-related fat deposition to channel fatty acids away from excessive oxidation.<sup>22,36</sup> This unique property enables *Pfkfb3* to dissociate adipose tissue inflammation from adiposity. As supporting evidence, global *Pfkfb3*-disrupted mice displayed increased severity of HFD-induced adipose tissue inflammation while revealing decreased adiposity.<sup>22</sup> In this line of mice, we examined NAFLD phenotype and demonstrated the dissociation of liver inflammation and hepatic steatosis. Of note, the increase in HFD-induced liver inflammation in global *Pfkfb3*-disrupted mice occurred in the presence of increased adipose tissue inflammation (reported previously in the study by Huo *et al.*<sup>22</sup>) whereas the absence of HFD-induced hepatic steatosis was accompanied with reduced adiposity. These findings indicated that *Pfkfb3* disruption, on the one side, exacerbated HFD-induced inflammation, and, on the other side, blunted or ameliorated HFD-induced fat deposition, *e.g.*, adiposity and hepatic steatosis. Because *Pfkfb3* is expressed at high abundance in both adipocytes and macrophages, the dissociation of inflammation and fat deposition was likely attributable to the differential roles played by the *Pfkfb3* in adipocytes versus macrophages. This notion, was based on, in large part, the findings from a gain-of-function study in which selective *Pfkfb3* overexpression in adipocytes significantly increased the severity of HFD-induced hepatic steatosis, but caused a significant decrease in liver inflammation.<sup>12</sup> The latter,

together with the results from global *Pfkfb3*-disrupted mice concerning NAFLD phenotype, suggest that intact *Pfkfb3* in adipocytes is a prerequisite for HFD feeding to induce adiposity, thereby hepatic steatosis. This speculation, indeed, is consistent with the finding that palmitoleate, whose production/release from adipocytes is increased in response to forced expression of *Pfkfb3*, acts to enhance hepatocyte lipogenesis and increase hepatic steatosis while suppressing hepatocyte proinflammatory responses.<sup>12</sup> As complementary evidence, *Pfkfb3* disruption in all cells, including adipocytes, blunted HFD-induced hepatic steatosis. Moreover, when *Pfkfb3* was intact in adipocytes, the chimeric mice in which *Pfkfb3* was disrupted only in hematopoietic cells revealed comparable amount of HFD-induced weight gain and adiposity compared with the chimeric mice in which *Pfkfb3* was intact in all cells. Given this, it is conceivable that *Pfkfb3* in nonhematopoietic cells, *e.g.*, adipocytes, is needed for HFD to induce hepatic steatosis in mice.

The common features of NAFLD between global *Pfkfb3*-disrupted mice and chimeric mice also validated the importance of *Pfkfb3* in suppressing HFD-induced liver inflammation. Specifically, when *Pfkfb3* was disrupted in all cells or only in hematopoietic cells, HFD-induced liver inflammation in the mice was significantly increased compared with that in the respective control mice whose *Pfkfb3* was intact. Considering that macrophages critically determine HFD-induced liver inflammation in mice,<sup>6,7,37</sup> we speculated that the *Pfkfb3* in macrophages plays an essential role in determining the degrees of liver inflammation. Indeed, this speculation was based on the findings from our recent study in which myeloid cell-specific *Pfkfb3* disruption exacerbated HFD-induced liver inflammation.<sup>23</sup> In the present study, the results from our chimeric mice demonstrated that *Pfkfb3* disruption only in hematopoietic cells increased the severity of HFD-induced liver inflammation. This serves as complementary evidence further validating the role for *Pfkfb3* in myeloid cells in protecting against HFD-induced liver inflammation. At the cellular level, *Pfkfb3* disruption increases macrophage proinflammatory activation and decreases macrophage anti-inflammatory activation. This regulation by *Pfkfb3* enables macrophages to critically regulate hepatocytes responses. As supporting evidence, hepatocytes co-cultured with *Pfkfb3*-disrupted macrophages revealed increased proinflammatory signaling, suggesting that macrophage factors generated in response to *Pfkfb3* disruption directly act to enhance hepatocyte proinflammatory responses. Collectively, *Pfkfb3* protection of liver inflammation is attributable to, in large part, suppression of macrophage proinflammatory activation. The latter, in turn, brings about decreases in the proinflammatory effects of macrophage-derived factors on hepatocyte inflammatory responses.

The *Pfkfb3* in macrophages also protects against the development of hepatic steatosis as this is supported by the findings from our recent study and by the data from the current study.<sup>23</sup> Specifically, *Pfkfb3* disruption in hematopoietic cells exacerbated the severity of HFD-induced hepatic steatosis. As substantial evidence, hepatocytes co-cultured with *Pfkfb3*-disrupted macrophages revealed an increase in palmitate-stimulated fat deposition. Given this, the role for *Pfkfb3* in macrophages in protecting against hepatic steatosis likely requires the presence of intact *Pfkfb3* in nonhematopoietic cells, *e.g.*, adipocytes. In other words, the *Pfkfb3* in macrophages appears to act through suppressing macrophage-derived pro-steatotic factors to protect against the development of hepatic steatosis, and this requires the conditions where hepatic steatosis can be induced. Consistent with this interpretation, in

global *Pfkfb3*-disrupted mice, *Pfkfb3* disruption in cells other than hematopoietic cells, presumably adipocytes, blunted the development of adiposity and acted to offset the pro-steatotic effect of *Pfkfb3* disruption in hematopoietic cells. This view warrants future investigation. Lastly, mast cells are also derived from hematopoietic cells and have been implicated to regulate the pathogenesis of NAFLD.<sup>38–40</sup> Considering this, it would be interesting to explore whether *Pfkfb3* also regulates the function of mast cells, thereby altering the development of hepatic steatosis and inflammation in future studies. Although not belonging to hematopoietic cells, hepatic stellate cells (HSCs) respond to macrophage-derived factors and are responsible for liver fibrosis. Given this, it would warrant future study to also address whether and how factors generated in response to *Pfkfb3* disruption in adipocytes versus macrophages differentially regulate the activation status of HSCs.

In summary, the present study provides evidence to support a unique role for *Pfkfb3* in regulating the aspects associated with NALFD. The notable finding is that *Pfkfb3* disruption only in hematopoietic cells exacerbated the severity of HFD-induced hepatic steatosis and inflammation whereas *Pfkfb3* disruption in all cells exacerbated liver inflammation but blunted hepatic steatosis. Because macrophage factors generated in response to *Pfkfb3* disruption acted to enhance hepatocyte fat deposition and proinflammatory responses, the *Pfkfb3* in macrophages is considered to critically protect against hepatic steatosis and inflammation. Moreover, intact *Pfkfb3* in nonhematopoietic cells, *e.g.*, adipocytes, appears to be needed for HFD feeding to induce hepatic steatosis, and for the *Pfkfb3* in hematopoietic cells to protect against HFD-induced hepatic steatosis. As such, the *Pfkfb3* in different cells plays differential roles in regulating the aspects of NAFLD.

## Acknowledgements

This work was supported in part by the Hickam Endowed Chair, Gastroenterology, Medicine, Indiana University and the Indiana University Health - Indiana University School of Medicine Strategic Research Initiative, the Research Career Scientist to Dr. Alpini from the United States Department of Veteran's Affairs, Biomedical Laboratory Research and Development Service and National Institutes of Health (NIH) grants DK054811, DK110035, and DK076898 to Drs. G. Alpini and S. Glaser. In addition, this work was supported in whole or in part by grants from the American Diabetes Association (ADA)(1-10-BS-76 to C. Wu) and the National Institutes of Health (DK095828 and DK124854 to C. Wu). C. Wu is also supported by the Hatch Program of the National Institutes of Food and Agriculture (NIFA). The views expressed in this article are those of the authors and do not necessarily represent the views of the Department of Veterans Affairs.

## References

1. Farrell GC, Larter CZ. Nonalcoholic fatty liver disease: from steatosis to cirrhosis. *Hepatology*. 2006;43:S99–S112. [PubMed: 16447287]
2. Estes C, Razavi H, Loomba R, Younossi Z, Sanyal AJ. Modeling the epidemic of nonalcoholic fatty liver disease demonstrates an exponential increase in burden of disease. *Hepatology*. 2018;67:123–133. [PubMed: 28802062]
3. Kodama Y, Kisseleva T, Iwaisako K, et al. c-Jun N-terminal kinase-1 from hematopoietic cells mediates progression from hepatic steatosis to steatohepatitis and fibrosis in mice. *Gastroenterology*. 2009;137:1467–1477 (e5). [PubMed: 19549522]
4. Pradere JP, Kluwe J, De Minicis S, et al. Hepatic macrophages but not dendritic cells contribute to liver fibrosis by promoting the survival of activated hepatic stellate cells in mice. *Hepatology*. 2013;58:1461–1473. [PubMed: 23553591]

5. Xu H, Li H, Woo SL, et al. Myeloid cell-specific disruption of Period 1 and Period 2 exacerbates diet-induced inflammation and insulin resistance. *J Biol Chem.* 2014;289:16374–16388. [PubMed: 24770415]
6. Cai Y, Li H, Liu M, et al. Disruption of adenosine 2A receptor exacerbates NAFLD through increasing inflammatory responses and SREBP1c activity. *Hepatology.* 2018;68:48–61. [PubMed: 29315766]
7. Luo X, Li H, Ma L, et al. Expression of STING is increased in liver tissues from patients with NAFLD and promotes macrophage-mediated hepatic inflammation and fibrosis in mice. *Gastroenterology.* 2018;155:1971–1984 (e4). [PubMed: 30213555]
8. Schwabe RF, Tabas I, Pajvani UB. Mechanisms of fibrosis development in nonalcoholic steatohepatitis. *Gastroenterology.* 2020;158:1913–1928. [PubMed: 32044315]
9. Xiong X, Kuang H, Ansari S, et al. Landscape of intercellular crosstalk in healthy and NASH liver revealed by single-cell secretome gene analysis. *Mol Cell.* 2019;75:644–660 (e5). [PubMed: 31398325]
10. Wang X, Rao H, Zhao J, et al. STING expression in monocyte-derived macrophages is associated with the progression of liver inflammation and fibrosis in patients with nonalcoholic fatty liver disease. *Lab Invest.* 2020;100:542–552. [PubMed: 31745210]
11. Speliotes EK, Massaro JM, Hoffmann U, et al. Fatty liver is associated with dyslipidemia and dysglycemia independent of visceral fat: the Framingham Heart Study. *Hepatology.* 2010;51:1979–1987. [PubMed: 20336705]
12. Huo Y, Guo X, Li H, et al. Targeted overexpression of inducible 6-phosphofructo-2-kinase in adipose tissue increases fat deposition but protects against diet-induced insulin resistance and inflammatory responses. *J Biol Chem.* 2012;287:21492–21500. [PubMed: 22556414]
13. Azzu V, Vacca M, Virtue S, Allison M, Vidal-Puig A. Adipose tissue-liver cross talk in the control of whole-body metabolism: implications in nonalcoholic fatty liver disease. *Gastroenterology.* 2020;158:1899–1912. [PubMed: 32061598]
14. Pei Y, Li H, Cai Y, et al. Regulation of adipose tissue inflammation by adenosine 2A receptor in obese mice. *J Endocrinol.* 2018;239:365–376. [PubMed: 30400017]
15. Monetti M, Levin MC, Watt MJ, et al. Dissociation of hepatic steatosis and insulin resistance in mice overexpressing DGAT in the liver. *Cell Metab.* 2007;6: 69–78. [PubMed: 17618857]
16. Puri P, Wiest MM, Cheung O, et al. The plasma lipidomic signature of nonalcoholic steatohepatitis. *Hepatology.* 2009;50:1827–1838. [PubMed: 19937697]
17. Lee JJ, Lambert JE, Hovhannisyanyan Y, et al. Palmitoleic acid is elevated in fatty liver disease and reflects hepatic lipogenesis. *Am J Clin Nutr.* 2015;101: 34–43. [PubMed: 25527748]
18. Guo X, Li H, Xu H, et al. Palmitoleate induces hepatic steatosis but suppresses liver inflammatory response in mice. *PLoS One.* 2012;7, e39286. [PubMed: 22768070]
19. Rider MH, Bertrand L, Vertommen D, Michels PA, Rousseau GG, Hue L. 6-phosphofructo-2-kinase/fructose-2,6-bisphosphatase: head-to-head with a bifunctional enzyme that controls glycolysis. *Biochem J.* 2004;381:561–579. [PubMed: 15170386]
20. Atsumi T, Nishio T, Niwa H, et al. Expression of inducible 6-phosphofructo-2-kinase/fructose-2,6-bisphosphatase/PFKFB3 isoforms in adipocytes and their potential role in glycolytic regulation. *Diabetes.* 2005;54:3349–3357. [PubMed: 16306349]
21. Okar DA, Wu C, Lange AJ. Regulation of the regulatory enzyme, 6-phosphofructo-2-kinase/fructose-2,6-bisphosphatase. *Adv Enzyme Regul.* 2004;44:123–154. [PubMed: 15581487]
22. Huo Y, Guo X, Li H, et al. Disruption of inducible 6-phosphofructo-2-kinase ameliorates diet-induced adiposity but exacerbates systemic insulin resistance and adipose tissue inflammatory response. *J Biol Chem.* 2010;285: 3713–3721. [PubMed: 19948719]
23. Ma L, Li H, Hu J, et al. Indole alleviates diet-induced hepatic steatosis and inflammation in a manner involving myeloid cell 6-phosphofructo-2-kinase/fructose-2,6-bisphosphatase 3. *Hepatology.* 2020. 10.1002/hep.31115.
24. Chesney J, Telang S, Yalcin A, Clem A, Wallis N, Bucala R. Targeted disruption of inducible 6-phosphofructo-2-kinase results in embryonic lethality. *Biochem Biophys Res Commun.* 2005;331:139–146. [PubMed: 15845370]

25. Woo SL, Xu H, Li H, et al. Metformin ameliorates hepatic steatosis and inflammation without altering adipose phenotype in diet-induced obesity. *PLoS One*. 2014;9, e91111. [PubMed: 24638078]
26. Cai D, Yuan M, Frantz DF, et al. Local and systemic insulin resistance resulting from hepatic activation of IKK-beta and NF-kappaB. *Nat Med*. 2005;11: 183–190. [PubMed: 15685173]
27. Payne VA, Arden C, Wu C, Lange AJ, Agius L. Dual role of phosphofructokinase-2/fructose bisphosphatase-2 in regulating the compartmentation and expression of glucokinase in hepatocytes. *Diabetes*. 2005;54:1949–1957. [PubMed: 15983194]
28. Bouhrel MA, Derudas B, Rigamonti E, et al. PPARgamma activation primes human monocytes into alternative M2 macrophages with anti-inflammatory properties. *Cell Metab*. 2007;6:137–143. [PubMed: 17681149]
29. Kang K, Reilly SM, Karabacak V, et al. Adipocyte-derived Th2 cytokines and myeloid PPARdelta regulate macrophage polarization and insulin sensitivity. *Cell Metab*. 2008;7:485–495. [PubMed: 18522830]
30. Odegaard JI, Ricardo-Gonzalez RR, Red Eagle A, et al. Alternative M2 activation of Kupffer cells by PPARdelta ameliorates obesity-induced insulin resistance. *Cell Metab*. 2008;7:496–507. [PubMed: 18522831]
31. Guo T, Woo SL, Guo X, et al. Berberine ameliorates hepatic steatosis and suppresses liver and adipose tissue inflammation in mice with diet-induced obesity. *Sci Rep*. 2016;6:22612. [PubMed: 26936230]
32. Coenen KR, Hasty AH. Obesity potentiates development of fatty liver and insulin resistance, but not atherosclerosis, in high-fat diet-fed agouti LDLR-deficient mice. *Am J Physiol Endocrinol Metab*. 2007;293:E492–E499. [PubMed: 17566116]
33. Clément S, Juge-Aubry C, Sgroi A, et al. Monocyte chemoattractant protein-1 secreted by adipose tissue induces direct lipid accumulation in hepatocytes. *Hepatology*. 2008;48:799–807. [PubMed: 18570214]
34. Milner KL, van der Poorten D, Xu A, et al. Adipocyte fatty acid binding protein levels relate to inflammation and fibrosis in nonalcoholic fatty liver disease. *Hepatology*. 2009;49:1926–1934. [PubMed: 19475694]
35. Qi L, Saberi M, Zmuda E, et al. Adipocyte CREB promotes insulin resistance in obesity. *Cell Metab*. 2009;9:277–286. [PubMed: 19254572]
36. Guo X, Xu K, Zhang J, et al. Involvement of inducible 6-phosphofructo-2-kinase in the anti-diabetic effect of peroxisome proliferator-activated receptor gamma activation in mice. *J Biol Chem*. 2010;285:23711–23720. [PubMed: 20498376]
37. Liang S, Ma HY, Zhong Z, et al. NADPH oxidase 1 in liver macrophages promotes inflammation and tumor development in mice. *Gastroenterology*. 2019;156: 1156–1172 (e6). [PubMed: 30445007]
38. Hargrove L, Kennedy L, Demieville J, et al. Bile duct ligation-induced biliary hyperplasia, hepatic injury, and fibrosis are reduced in mast cell-deficient Kit<sup>W-sh</sup> mice. *Hepatology*. 2017;65:1991–2004. [PubMed: 28120369]
39. Meng F, Kennedy L, Hargrove L, et al. Ursodeoxycholate inhibits mast cell activation and reverses biliary injury and fibrosis in Mdr2<sup>-/-</sup> mice and human primary sclerosing cholangitis. *Lab Invest*. 2018;98:1465–1477. [PubMed: 30143751]
40. Lombardo J, Broadwater D, Collins R, Cebe K, Brady R, Harrison S. Hepatic mast cell concentration directly correlates to stage of fibrosis in NASH. *Hum Pathol*. 2019;86:129–135. [PubMed: 30597154]

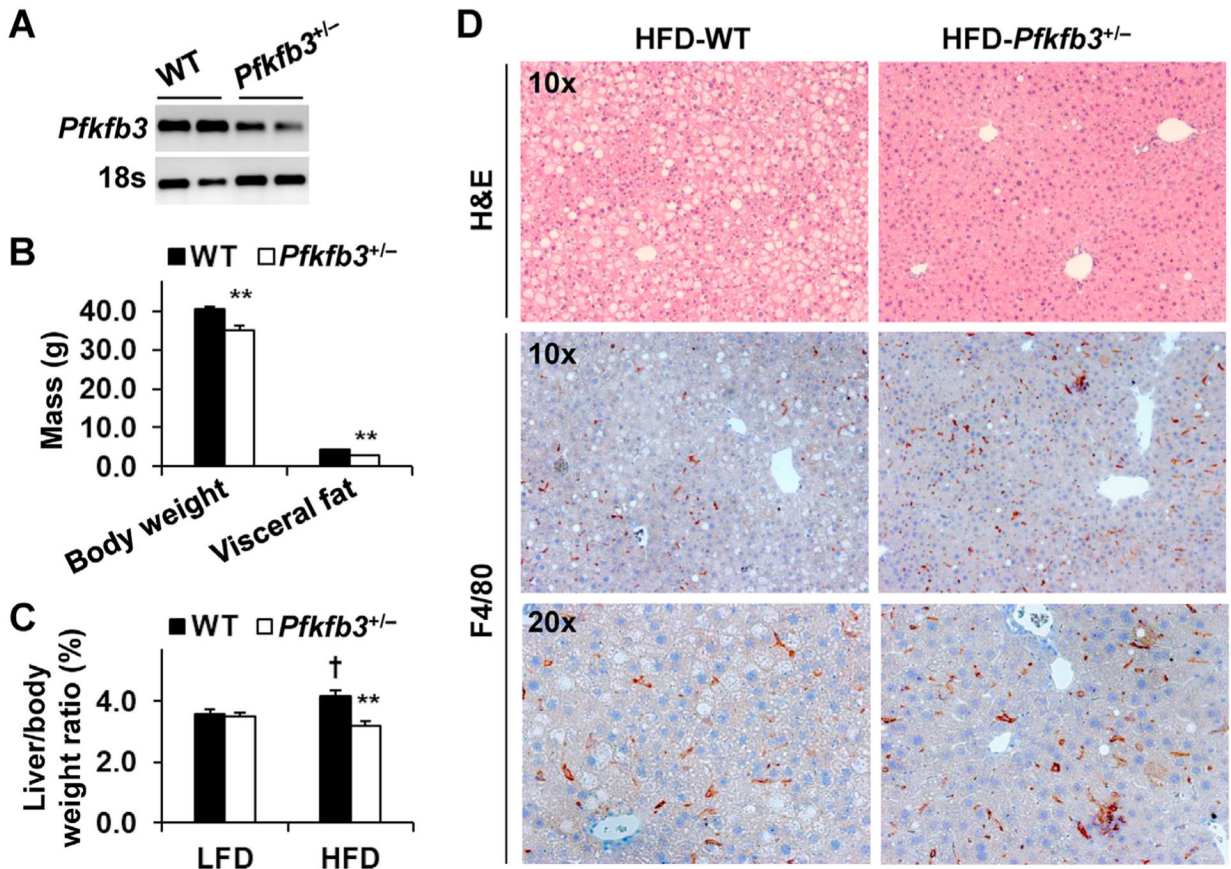


**Fig. 1. Global *Pfkfb3* disruption blunts HFD-induced hepatic steatosis but increases liver macrophage accumulation.**

Global heterozygous *Pfkfb3*-disrupted (*Pfkfb3*<sup>+/-</sup>) mice and WT (*Pfkfb3*<sup>+/+</sup>) littermates were described in Materials and methods. (A) Validation of *Pfkfb3* disruption. Tail deoxyribonucleic acid (DNA) was examined for *Pfkfb3* expression using polymerase chain reaction (PCR). (B) Body weight and visceral fat mass ( $N = 10$  for body weight and  $N = 7$  for fat mass). (C) Liver/body weight ratios ( $N = 7$ ). (D) Liver histology. Liver sections were stained with H&E or for F4/80 expression. For B–D, *Pfkfb3*<sup>+/-</sup> mice and WT littermates, at 5–6 weeks of age, were fed HFD (60% fat calories) or LFD (10% fat calories) for 12 weeks. At the end of feeding period, mice were fasted for 4 h prior to harvest. For B and C, data are means  $\pm$  SEM. \*\*,  $P < 0.01$  *Pfkfb3*<sup>+/-</sup> vs. WT in B for the same type of mass or in C on the same diet; †,  $P < 0.05$  HFD vs. LFD for the same genotype. Abbreviations: H&E, hematoxylin and eosin; HFD, high-fat diet; LFD, low-fat diet; *Pfkfb3*, 6-phosphofructo-2-kinase/fructose-2,6-biphosphatase 3; WT, wild-type.

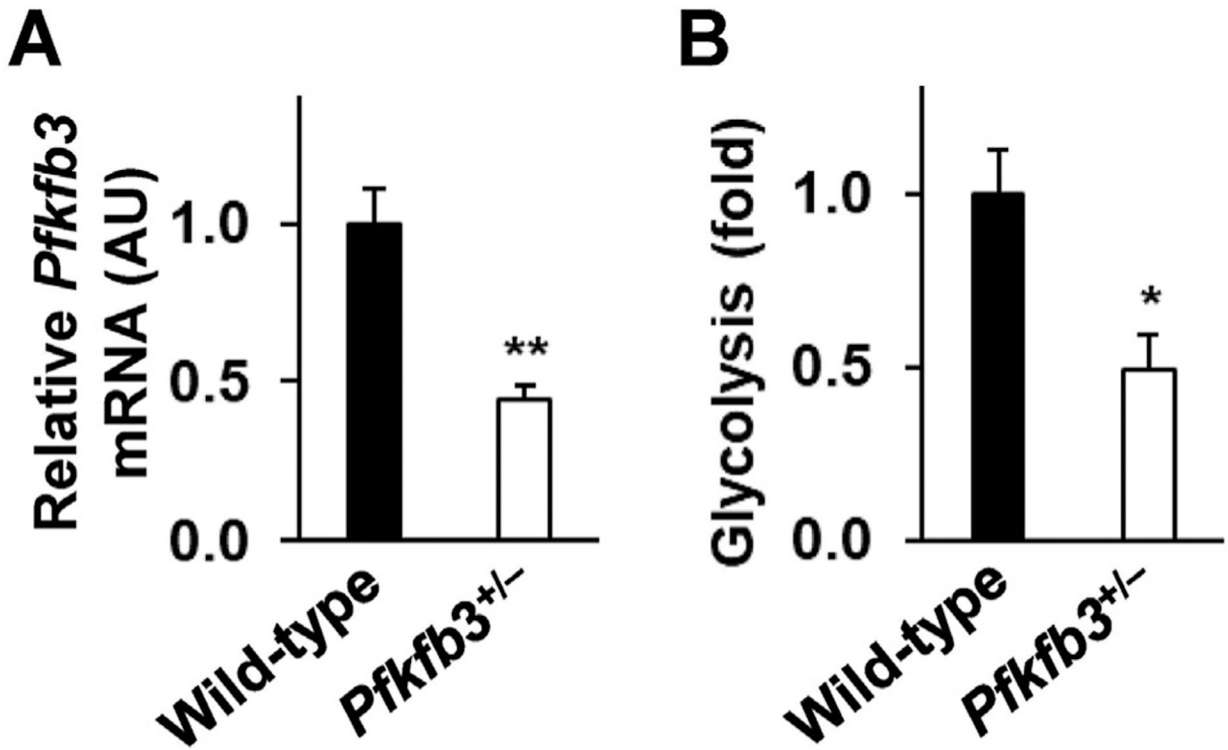


**Fig. 2. *Pfkfb3* disruption decreases the rates of glycolysis.**

Bone marrow cells were isolated from male *Pfkfb3*-disrupted (*Pfkfb3*<sup>+/-</sup>) mice and WT (*Pfkfb3*<sup>+/+</sup>) littermates, at 10–12 weeks of age, and differentiated into macrophages (BMDMs). (A) Macrophage *Pfkfb3* mRNA levels. After harvest, the mRNA levels of *Pfkfb3* were examined using real-time PCR. (B) Macrophages glycolysis rates. Prior to harvest, BMDMs were incubated with <sup>3</sup>H-glucose (1  $\mu$ Ci/3 mL) for 3 h. Rates of glycolysis were calculated as the generation of <sup>3</sup>H<sub>2</sub>O per mg cell proteins. For A and B, data are means  $\pm$  SEM.  $N = 4$  (WT) and 6 (*Pfkfb3*<sup>+/-</sup>). \*,  $P < 0.05$  and \*\*,  $P < 0.01$  *Pfkfb3*<sup>+/-</sup> vs. Wild-type. Abbreviations: AU, arbitrary unit; BMDMs, bone marrow-derived macrophages; *Pfkfb3*, 6-phosphofructo-2-kinase/fructose-2,6-biphosphatase 3; WT, wild-type.

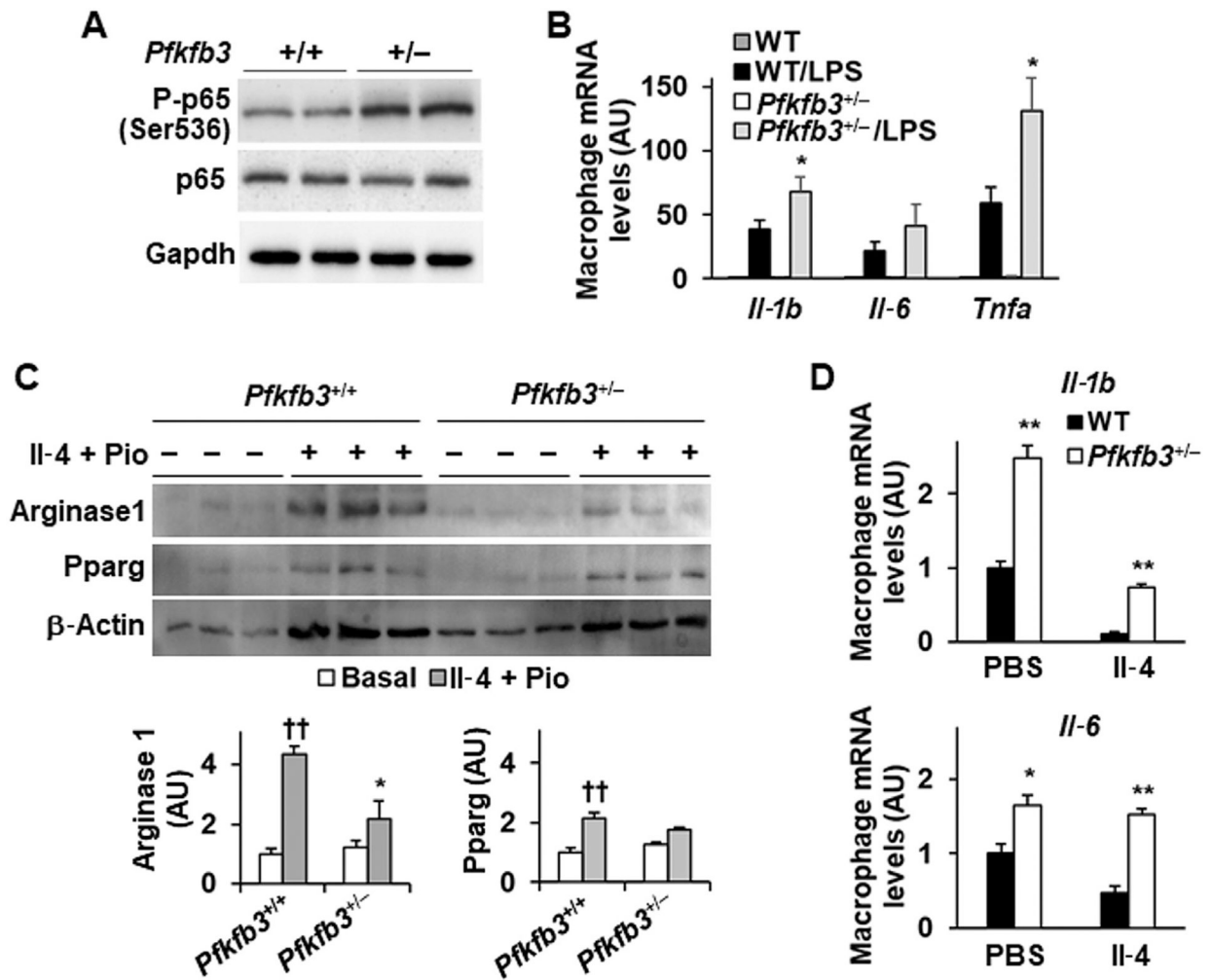


**Fig. 3. *Pfkfb3* disruption exacerbates macrophage proinflammatory activation and impairs macrophage anti-inflammatory activation.**

Bone marrow cells were isolated from male *Pfkfb3*-disrupted (*Pfkfb3*<sup>+/-</sup>) mice and WT (*Pfkfb3*<sup>+/+</sup>) littermates, at 10–12 weeks of age, and differentiated into macrophages (BMDMs). (A) Macrophage proinflammatory signaling. After harvest, cell lysates were examined for total protein and the phosphorylation states of Nfkb p65 using Western blot analysis. Representative blots from 4 WT to 6 *Pfkfb3*-disrupted mice. (B) Macrophage cytokine expression. BMDMs were treated with or without LPS (20 ng/mL) for 6 h prior to harvest. *N* = 4 (WT) and 6 (*Pfkfb3*<sup>+/-</sup>). (C) Changes in macrophage alternative activation markers. BMDMs were treated with or without Il-4 (10 ng/mL) in the presence or absence of pioglitazone (Pio, 1 μM) for 48 h. Cell lysates were subjected to Western blot analysis. *N* = 3. (D) Prior to harvest, BMDMs were treated with or without Il-4 (10 ng/mL) for 48 h. The expression of cytokines was analyzed using real-time PCR. Data are means ± SEM. *N* = 4 (WT) and 6 (*Pfkfb3*<sup>+/-</sup>). \*, *P* < 0.05 and \*\*, *P* < 0.01 *Pfkfb3*<sup>+/-</sup> vs. WT with the same treatment (Il-4 or PBS). Abbreviations: AU, arbitrary unit; Il-1b, interleukin-1beta; LPS, lipopolysaccharide; Pfkfb3, 6-phosphofructo-2-kinase/fructose-2,6-biphosphatase 3; Pio, pioglitazone; Pparg, peroxisome proliferator-activated receptor gamma; Tnfa, tumor necrosis factor alpha; WT, wild-type.

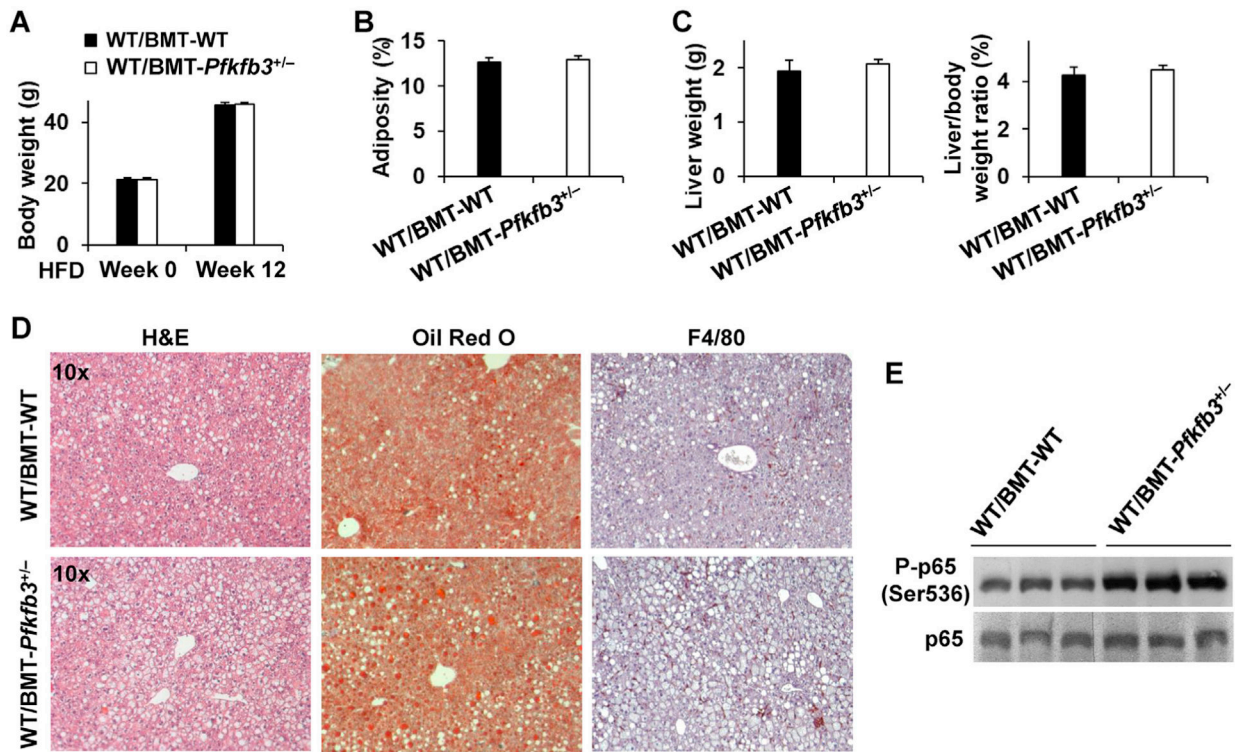


**Fig. 4. Adoptive transfer of *Pfkfb3*-disrupted bone marrow cells to WT recipient mice exacerbates NAFLD phenotype without altering body and adiposity.**

Bone marrow cells from *Pfkfb3*-disrupted (*Pfkfb3*<sup>+/-</sup>) mice and/or WT littermates were transplanted into lethally irradiated male WT mice, at 5–6 weeks of age (BMT). After recovery for 4 weeks, chimeric mice were fed an HFD (60% fat calories) for 12 weeks. WT/BMT-*Pfkfb3*<sup>+/-</sup>, WT mice were transplanted with bone marrow cells from *Pfkfb3*<sup>+/-</sup>; WT/BMT-WT, WT mice were transplanted with WT bone marrow cells. (A) Body weight of the chimeric mice before and after HFD feeding ( $N = 10$ ). (B) Adiposity of chimeric mice after HFD feeding ( $N = 7$ ). (C) Liver weight ( $N = 7$ ). (D) Liver histology and immunohistochemistry. Left panels, liver sections were stained with H&E; middle panels, liver sections were stained with Oil Red O; right panels, liver sections were stained for F4/80 expression. (E) Representative images for changes in liver Nfkb p65 phosphorylation states. Liver lysates were prepared from 3 randomly selected mice per group and subjected to Western blot analysis. For bar graphs in A–C, data are means  $\pm$  SEM. Abbreviations: BMT, bone marrow transplantation; H&E, hematoxylin and eosin; HFD, high-fat diet; *Pfkfb3*, 6-phosphofructo-2-kinase/fructose-2,6-biphosphatase 3; WT, wild-type.

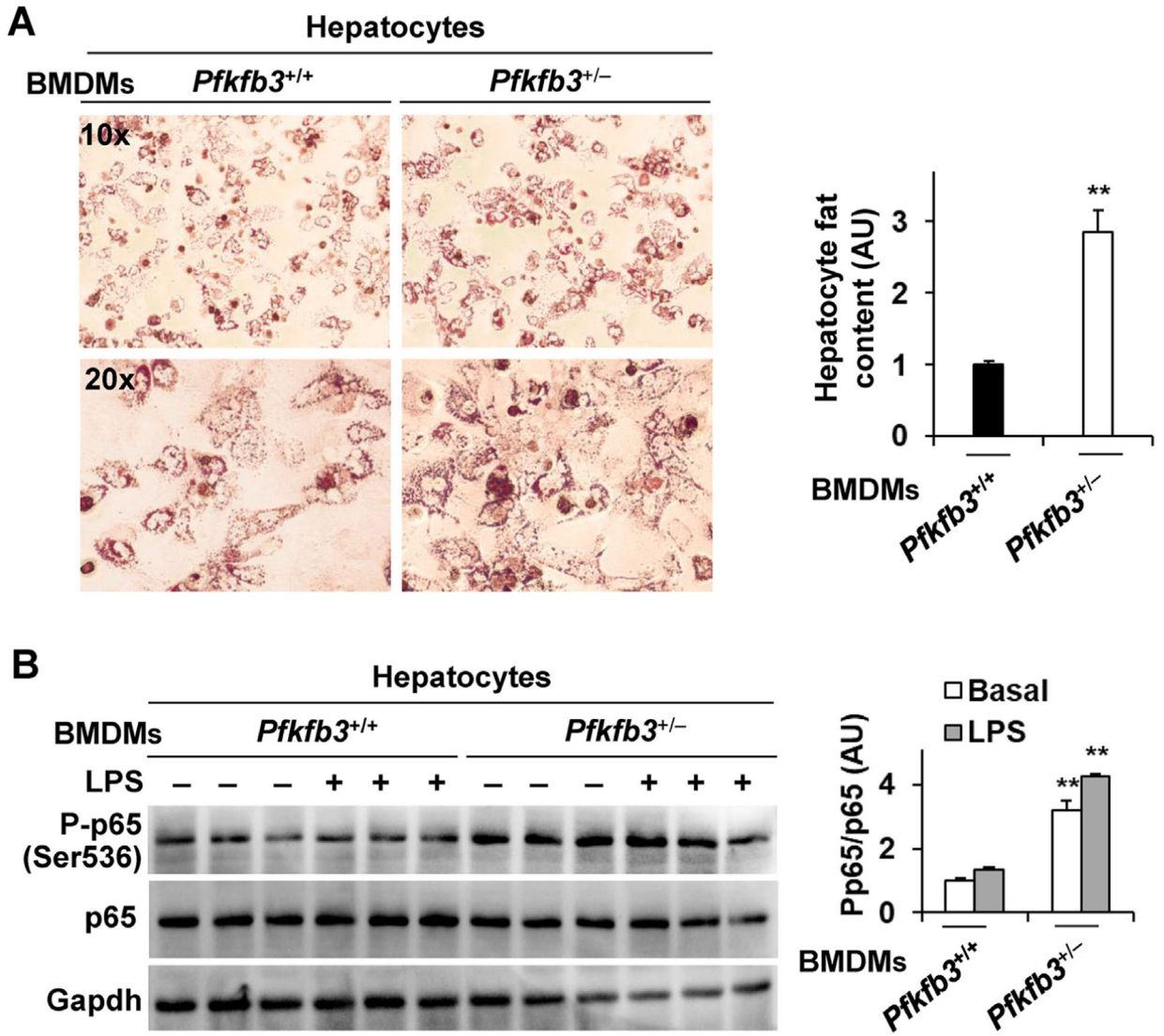


**Fig. 5. *Pfkfb3*-disrupted macrophages increased hepatocyte fat deposition and proinflammatory signaling.**

Bone marrow cells were isolated from male *Pfkfb3*-disrupted (*Pfkfb3*<sup>+/-</sup>) mice and/or WT littermates, at 10–12 weeks of age, and differentiated into macrophages (BMDMs). Primary hepatocytes were isolated from male WT mice, at 10–12 weeks of age. After overnight incubation, primary hepatocytes were co-cultured with BMDMs at a 10:1 ratio for 48 h. (A) Hepatocyte fat deposition. Prior to harvest, the co-cultures were treated with palmitate (250 μM) for 24 h and stained with Oil Red O for the last 1 h. Bar graph, quantification of hepatocyte fat content. (B) Hepatocyte proinflammatory signaling. Prior to harvest, the co-cultures were treated with or without LPS (100 ng/mL) for the last 30 min. Bar graph, quantification of blots. For A and B, numeric data are means ± SEM. *N* = 4 (hepatocytes co-cultured with WT BMDMs) and 6 (hepatocytes co-cultured with *Pfkfb3*<sup>+/-</sup> BMDMs). \*\*, *P* < 0.01 hepatocytes co-cultured with *Pfkfb3*<sup>+/-</sup> BMDMs vs. hepatocytes co-cultured with *Pfkfb3*<sup>+/+</sup> BMDMs (in A under palmitate-stimulated condition and in B under Basal or LPS-stimulated condition). Abbreviations: AU, arbitrary unit; BMDMs, bone marrow-

derived macrophages; LPS, lipopolysaccharide; Pfkfb3, 6-phosphofructo-2-kinase/fructose-2,6-biphosphatase 3; WT, wild-type.

Author Manuscript

Author Manuscript

Author Manuscript

Author Manuscript

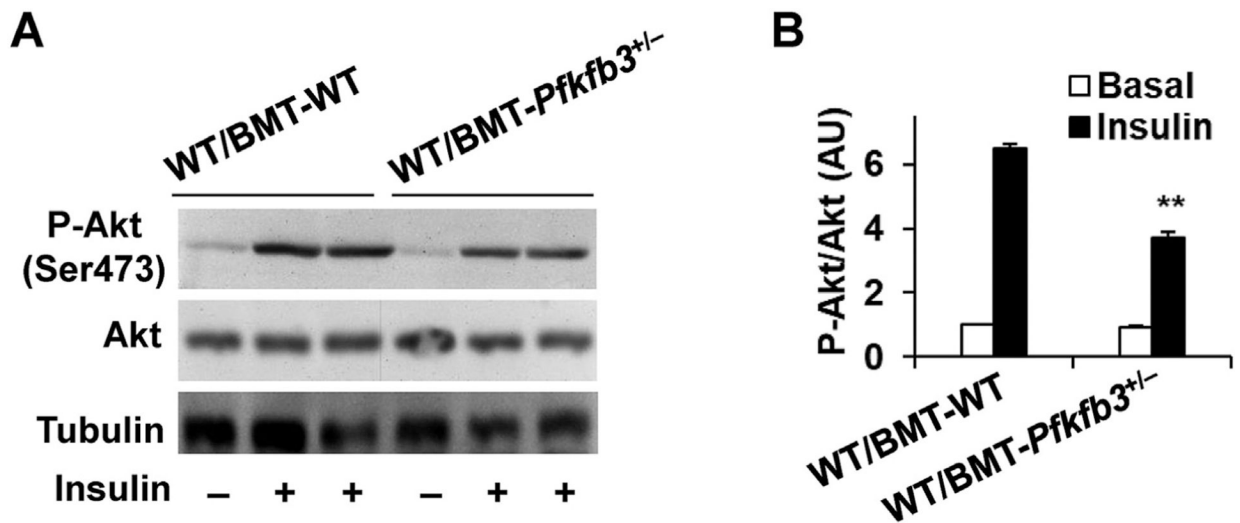


**Fig. 6.**

Adoptive transfer of *Pfkfb3*-disrupted bone marrow cells to WT recipients impairs hepatic insulin signaling. Chimeric mice were described in Fig. 4. WT/BMT-*Pfkfb3*<sup>+/-</sup>, WT mice were transplanted with bone marrow cells from *Pfkfb3*<sup>+/-</sup>; WT/BMT-WT, WT mice were transplanted with WT bone marrow cells. Prior to harvest, HFD-fed mice were subjected to a bolus injection of insulin (1 U/kg) into the portal vein for 5 min. Liver lysates were examined for the total and phosphorylation states of Akt using Western blot analysis. **(A)** Representative blots. Liver samples were prepared from 3 WT or *Pfkfb3*<sup>+/-</sup> mice in the absence of insulin injection and 4 WT or *Pfkfb3*<sup>+/-</sup> mice received insulin injection. **(B)** Quantification of blots. Data are means  $\pm$  SEM.  $N = 3$  (without insulin) and 4 (with insulin). \*\*,  $P < 0.01$  WT/BMT-*Pfkfb3*<sup>+/-</sup> vs. WT/BMT-WT under insulin-stimulated condition. Abbreviations: AU, arbitrary unit; BMT, bone marrow transplantation; *Pfkfb3*, 6-phosphofructo-2-kinase/fructose-2,6-biphosphatase 3; WT, wild-type.